

model. The program runs more slowly, but the present tapered-wing version should certainly be competitive with integral methods needing several spanwise stations.

To a good approximation (neglecting the effect of the spanwise variation of Reynolds number based on chord) δ at given x is proportional (Fig. 1) to $r_0 - z$ and, for any function f , $\partial f / \partial z$ at constant y is equal to $y/r_0 \partial f / \partial y$. Thus in the transport equation for f , $V \partial f / \partial y$ and $W \partial f / \partial z$ combine to yield $(V + Wy/r_0) \partial f / \partial y$. As in Ref. 9, $\bar{\rho} V$ is augmented by the turbulent mass flux in the y direction, $\bar{\rho}' v$. If we denote $V + \bar{\rho}' v / \bar{\rho} + Wy/r_0$ by \hat{V} the equations for u , \hat{V} , W , $-\bar{\rho} u v$ and $-\bar{\rho} w v$ are the same as for an infinite wing except for the rotation of axes terms.

The program contains a large number of options for input, output, and physical effects, selected individually by choosing nonzero values of integer control parameters so that default operation is obtained with two essential control parameters and a row of blanks.⁷ The number of y profile points must be chosen by the user, but in general the program is no more complicated to use than an integral method. Aerodynamic options include surface roughness¹¹ and allowances for the effects of surface curvature,¹² lateral convergence/divergence, bulk dilatation¹³ and freestream turbulence on the turbulence structure. The program contains just under 1000 Fortran statements, executes in 8,500 (decimal) words plus computer library space and marches in the x direction at about 8 boundary-layer thicknesses per second on a CDC 6400 (this is about two-thirds the speed of the two-dimensional compressible heat transfer program or half the speed of the incompressible isothermal program).

The empirical data used by the program are all obtained from two-dimensional flow; with the exception of the allowance for bulk dilatation effects and the effect of Mach number on the additive constants in the logarithmic inner-layer profiles, the data all come from incompressible flow and those of Ref. 9 and 13 in two-dimensional compressible flow, while in the later case, the Reynolds analogy factor in constant-pressure flow is close to 1.16. The results in zero pressure gradient are acceptable up to a freestream Mach number M_e of at least 10 although the Morkovin hypothesis¹⁴ justifying the turbulence modeling requires that the local Mach number M shall satisfy $(\gamma - 1)M^2 \gg 1$. The Reynolds analogy factor in constant-pressure flow remains close to 1.16 over the range $0.25 < T_w/T_{oe} < 4$. There is no explicit limit on sweep angle, but the assumption of radial isobars and the neglect of influence spreading through the boundary layer from other parts of the wing are likely to fail in many cases where the sweep angle exceeds, say, 45° and are certain to fail in most cases near the root and tip of the wing. It is likely that the assumption (which can be checked) will in practice fail before the neglect (which cannot). The program will run to within one x step of separation: van den Berg et al.¹⁵ have recently found discrepancies between existing calculation methods (including the present one) and their measurements of a separating boundary layer on an infinite yawed wing, but it is not clear that the discrepancies are connected with the three-dimensionality.

Fortran card decks are available from the first author for the cost of reproducing and mailing. Subsets of the full program, e.g., two-dimensional compressible heat transfer, are also available.

References

- Thompson, B. G. J., Carr-Hill, G. A., and Ralph, M., "The Prediction of Boundary-Layer Behavior and Profile Drag for Infinite Yawed Wings. Part III," CP 1309, 1973, Aeronautical Research Council, London, England.
- Bradshaw, P., "Calculation of Three-Dimensional Turbulent Boundary Layers," *Journal of Fluid Mechanics*, Vol. 46, 1971, p. 417.
- Cebeci, T., Mosinskis, G. J., and Kaups, K., "A General Method for Calculating Three-Dimensional Incompressible Laminar and Tur-

bulent Boundary Layers. I," Douglas Aircraft Co., MDC J5694, 1972.

⁴Adams, J. C., "Calculation of Compressible Turbulent Boundary Layers on an Infinite Yawed Aerofoil," *Journal of Spacecraft*, Vol. 12, 1975, p. 131.

⁵Rodi, W., "Basic Equations for Turbulent Flow in Cartesian and Polar Coordinates," Imperial College, BL/TN/A/36, 1970, and Corrigenda, 1971.

⁶Nash, J. F. and Scruggs, R. M., "Three Dimensional Compressible Boundary Layer Computations for a Finite Swept Wing," CR-112158, 1972, NASA.

⁷Bradshaw, P. and Unsworth, K., "An Improved Fortran Program for the Bradshaw-Ferriss-Atwell Method of Calculating Turbulent Shear Layers," Aero Rept. 74-02, 1974, Imperial College, London.

⁸Bradshaw, P. and Ferriss, D. H., "Applications of a General Method of Calculating Turbulent Shear Layers," *Transactions of the ASME Basic Engineering*, Vol. 94D, 1972, p. 345.

⁹Bradshaw, P. and Ferriss, D. H., "Calculation of Boundary Layer Development Using the Turbulent Energy Equation. Compressible Flow on Adiabatic Walls," *Journal of Fluid Mechanics*, Vol. 46, 1971, p. 83.

¹⁰Bradshaw, P., Mizner, G. A., and Unsworth, K., "Calculation of Compressible Turbulent Boundary Layers with Heat Transfer on Straight-Tapered Swept Wings," Aero Rept. 75-04, 1975, Imperial College, London.

¹¹Goddard, F. E., "Effect of Uniformly-Distributed Roughness on Turbulent Skin-Friction Drag at Supersonic Speeds," *Journal of Aeronautical Science*, Vol. 26, 1959, p. 1.

¹²Bradshaw, P., "Effect of Streamline Curvature on Turbulent Flow," AGARDograph 169, 1973.

¹³Bradshaw, P., "The Effect of Mean Compression or Dilatation on the Turbulence Structure of Supersonic Boundary Layers," *Journal of Fluid Mechanics*, Vol. 63, 1974, p. 449.

¹⁴Morkovin, M. V., "Effects of Compressibility on Turbulent Flows," *The Mechanics of Turbulence*, A. Favre, ed., Gordon & Breach, New York, 1964, p. 367.

¹⁵Van den Berg, B., Elsenaar, A., Lindhout, J., and Wesseling, P., "Measurements in an Incompressible Three-Dimensional Turbulent Boundary Layer, under Infinite Swept Wing Configurations, and Comparison with Theory," *Journal of Fluid Mechanics*, Vol. 70, 1975, p. 127.

Effect of Velocity Gradients on Measurements of Turbulent Shear Stress

V.A. Sandborn*

Colorado State University, Fort Collins, Colo.

Introduction

IN a recent Note Johnson and Rose¹ demonstrated that both laser velocimeter and hot wire measurements obtained in a supersonic boundary layer fail to give the expected values of the turbulent shear stress near the surface. In the outer portion of the boundary layer both instruments agree approximately with the general flat plate similarity shear distribution proposed by Sandborn.² While a question on the use of $\bar{\rho} u v$ as the total shear stress was posed by Johnson and Rose, it is likely that a probe measurement difficulty exists near the surface.

Measurements in regions of large mean and turbulent velocity gradients can produce correspondingly large errors. For the boundary layer studied by Johnson and Rose, the thickness was of the order of 2.5 cm, with the mean velocity varying from zero to 550 m/sec over this short distance. The

Received September 29, 1975; revision received December 1, 1975. The author gratefully acknowledges the support of the NASA-Ames Research Center in the research.

Index category: Boundary Layer and Convective Heat Transfer-Turbulent.

*Professor of Civil Engineering. Member AIAA.

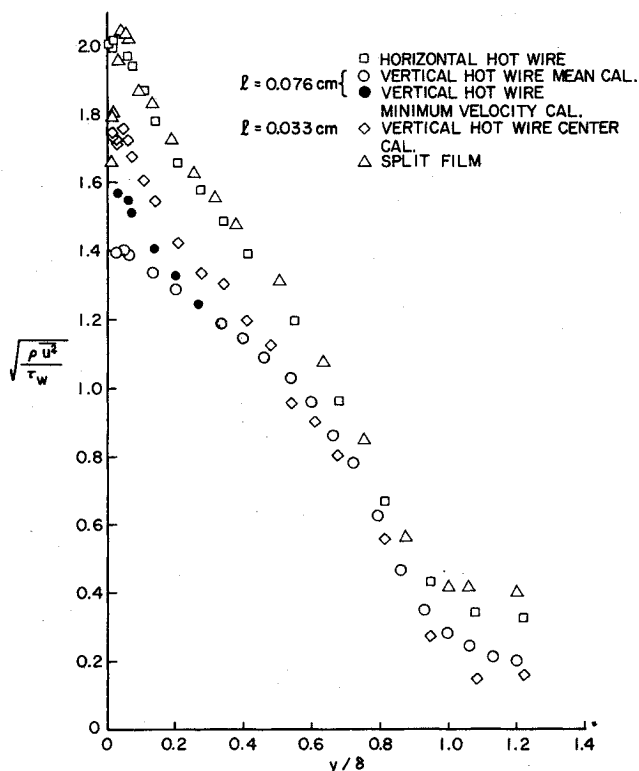


Fig. 1 Longitudinal turbulent velocity evaluation.

gradient is largest at and near the surface. The measuring instruments, both the laser and hot wire, have a finite length in the vertical direction (.13cm yawed wire, or approximately .06cm in the vertical direction). Very near the surface the mean velocity across the yawed wire could vary by as much as 100 m/sec. The problem can be further complicated by the presence of gradients in both the longitudinal and vertical turbulent velocity components.

Experimental evaluation of the velocity gradient effect on hot wires was reported by Tielman and Sandborn^{3,4} for a thick, low speed, turbulent boundary layer (70cm thick). For this flow the mean velocity gradient was small, and the turbulent gradient appeared to be the more important effect. The present Note demonstrates the effects of normal velocity gradients on hot wire measurements in a subsonic boundary layer of the same size as the flow investigated by Johnson and Rose.¹ The results demonstrate that major errors are encountered due to the gradients.

Experimental Study

The measurements were made 282cm downstream from the inlet of a 10.2-by-15.2cm, smooth aluminum channel.⁵ The flow is accelerating and approaching a fully developed channel flow. The nominal measured boundary layer parameters were: edge Mach No. 0.22, boundary layer thickness 3.8cm, and momentum thickness Reynolds No. 16400. Velocity and pressure distributions for the flow are reported in Ref. 5. The study was made at a Mach number of 0.22, so that density and temperature fluctuations could be neglected.

Both hot wire and film anemometers were used to measure the boundary layer turbulent properties. Platinum-8% tungsten, 0.001cm diam, hot wires were used. A commercial "split film" probe, 0.015cm in diameter was also evaluated.⁶ A special X-wire probe with one wire vertical and the second wire at an angle of approximately 40° to the flow was used to demonstrate the gradient effects. Although the overall error of this special X-probe, will not be the same as that of the convectional X-probe, the vertical wire indicates directly the error due to the gradients.

Figure 1 compares the measurements of the longitudinal turbulent component $(\bar{u}^2)^{1/2}$ made with a horizontal hot wire,

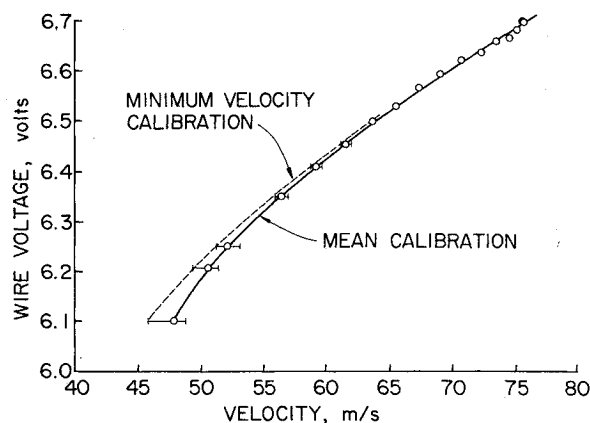


Fig. 2 Vertical hot wire calibration in the boundary layer.

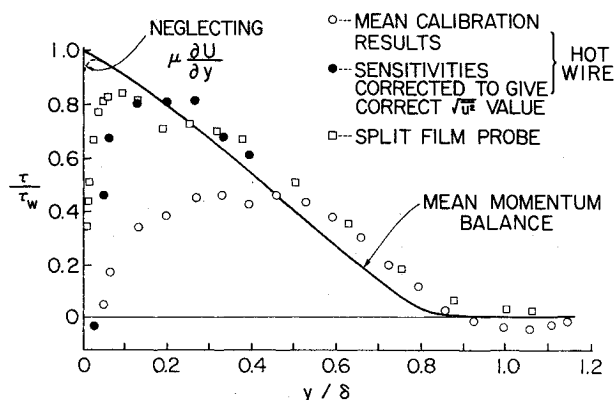


Fig. 3 Turbulent shear stress evaluation with a X-wire, hot wire and a split film probe.

two different length vertical hot wires, and the split film probe. The horizontal hot wire was assumed to be a good estimate of the actual value of $(\bar{u}^2)^{1/2}$. The vertical hot wire values are in error due to the velocity gradients along their length. Figure 2 shows the mean voltage output versus the mean velocity at the center of the 0.076cm vertical wire as it was traversed across the boundary layer. The mean velocity was evaluated independently with a total pressure probe. The "bars" shown on Fig. 2 indicate the variation in velocity across the wire length. Both the mean and minimum curves drawn on Fig. 2 were employed to evaluate $(\bar{u}^2)^{1/2}$, as noted on Fig. 1. The shorter wire ($\ell=0.033$ cm) data on Fig. 1 was evaluated only from a mean flow calibration.

The split film results agree closely with the horizontal wire values. Only very close to the wall was a deviation noted. The longitudinal component was evaluated assuming the sum of the heat transfer from the 2 films was a function of the mean velocity only.⁵ A slight dependency on the yaw angle was observed (ratio of vertical to longitudinal velocity sensitivity ≈ 0.18), however, it proved to be neglectable for the present measurements. A special rotation mount was employed to evaluate the angle sensitivity.

The major difficulty in hot wire measurements is the evaluation of the turbulent shear stress, since a vertical yawed wire must be used to sense the v -component. Figure 3 shows the evaluation of \bar{uv} made with the X-wire and split film probes. A momentum balance was made from mean velocity and pressure measurements⁵ to determine the total shear stress distribution shown on Fig. 3. The probe measurements were taken slightly downstream (10cm) of the point where the balance was made.

Use of calibration curves for the vertical and yawed wires of the $\ell=0.076$ cm probe, obtained from the mean velocity traverses (shown for the vertical wire on Fig. 2), resulted in the open circles shown on Fig. 3. The technique of evaluating the X-wire data is discussed in Ref. 5. The disagreement of the

measured and expected values of shear stress near the surface is quite large. A "correction" that increases the vertical wire sensitivity to that necessary to force a correct value for the u -component was applied to both the vertical and yawed wires.⁴ The correction (shown as the solid points on Fig. 3) was an improvement in the agreement, but still not adequate. It is not obvious that one could expect the sensitivity of the yawed wire to be affected identically to that of the vertical wire. For the case of the low speed boundary layer,³ where the turbulence gradients were more important, this form of correction was reasonable. As opposed to the present results, the uncorrected low speed results gave too great a value of uv near the wall.

Figure 3 also shows the split film probe measure of the shear stress. The output was evaluated by assuming each film can be treated similar to a yawed hot wire.⁵ Attempts to employ the difference or the ratio of the heat transfer from the two films⁶ were abandoned, since these functions were found to depend both on flow direction and velocity. The split film results indicate an improvement in the evaluation of uv over that of the X -wire. However, the gradient problem is still important near the surface. It is doubtful that the probe size can be further reduced to completely overcome the gradient effects at high speeds.

Conclusions

It is demonstrated that major errors are encountered when mean and turbulent velocity gradients exist along the length of hot wire sensors. Although the problem is also present in low speed measurements it is more pronounced at the high speeds. For the present case evaluated the errors are too great to be corrected accurately. Although the split film sensor results showed a significant improvement over the X -wire sensor results, further reduction in the space resolution of sensors by approximately an order of magnitude would appear to be necessary to reduce the error to acceptable values near the wall.

References

- Johnson, D.A. and Rose, W.C., "Laser Velocimeter and Hot-Wire Anemometer Comparison in a Supersonic Boundary Layer," *AIAA Journal*, Vol. 13, April 1975, pp. 512-515.
- Sandborn, V.A., "A Review of Turbulence Measurements in Compressible Flow," NASA TM X-62,337, March 1974.
- Tielman, H.W. and Sandborn, V.A., "Turbulent Shear Measurements in Large Velocity Gradients," Colorado State Univ. Engineering Report CER67-68HWT-VAS68, 1968, Fort Collins, Colo.
- Sandborn, V.A., *Resistance Temperature Transducers*, Metrology Press, Fort Collins, Colo. 1972, p. 294.
- Sandborn, V.A. and Seegmiller, H.L., "Evaluation of Mean and Turbulent Velocity Measurements in Subsonic, Accelerated Boundary Layers," NASA TM X-62, 488, Sept. 1975.
- Spencer, B.W., and Jones, B.G., "Turbulence Measurements with the Split Film Anemometer Probe," *Proceedings of the Symposium of Turbulence in Liquids*, Univ. of Missouri-Rolla, Rolla, Mo. 1971.

Production of Diamonds from Graphite Using Explosive-Driven Implosions

I.I. Glass* and S.P. Sharma†
University of Toronto, Toronto, Canada

Introduction

NATURAL diamonds have been used by man since antiquity as charms and ornamental objects. Its al-

Received Nov. 12, 1975. The financial support from the National Research Council of Canada and the U.S. Air Force under Grant No. AF-AFOSR 72-2274C is acknowledged with thanks.

Index categories: Multiphase Flows; Shock Waves and Detonations; Hypervelocity Impact.

*Professor, Institute for Aerospace Studies. Fellow AIAA.

†Research Assistant, Institute for Aerospace Studies.

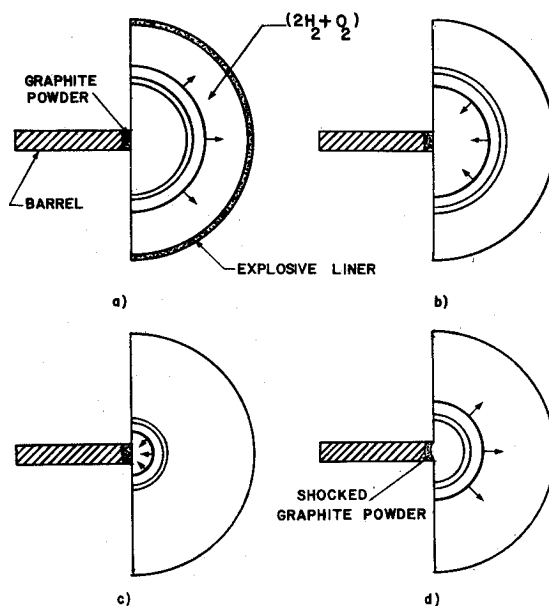


Fig. 1 Operation of UTIAS implosion chamber facility. a) Ignition and outgoing detonation wave. b) Detonation of explosive liner and detonation wave reflection. c) Strong imploding shock wave. d) Imploding shock wave reflection and compression of graphite powder at the origin.

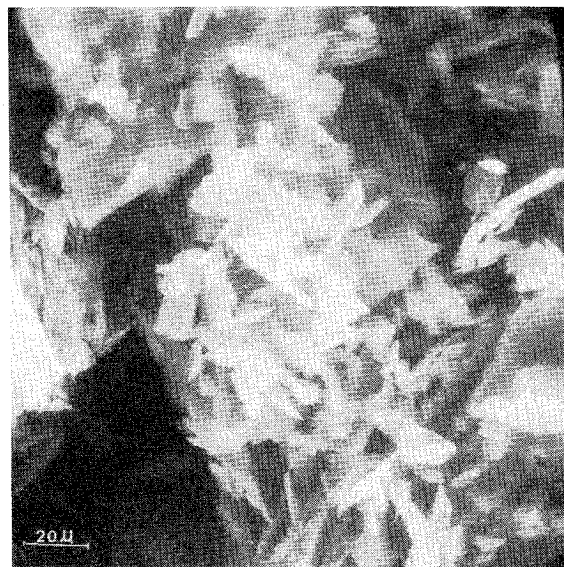


Fig. 2 Scanning electron micrograph of unshocked graphite powder (8400 \times).

lotropic form of carbon was established by Tennant in 1797,¹ and led to several attempts to produce it synthetically. However, it was not until 1954 that synthetic diamonds, in the 100- to 1000- μ range, finally were produced at General Electric by Bundy et al.² They applied a large hydraulic press ($> 50,000$ atm) for about 5 min to a graphite cartridge that was heated simultaneously to high temperatures ($> 2000^\circ$ K) by an electric current. Such physical conditions³ were not attainable before in the laboratory, and this prevented the early experimenters from synthesizing diamonds from carbon. In 1961, diamonds were produced by explosive shock compression and heating of graphite powder in a cartridge.⁴ In this case, the pressures of 200 to 300 kbar were applied only for microseconds in order to produce diamond aggregates of 0.05 to 0.1 μ . The foregoing types of processes now are used commercially for producing industrial diamonds suitable for lapping and polishing.

Diamonds also have been produced by using multipoint detonators to initiate a spherical shell of explosive, thereby